THE ASTROPHYSICAL JOURNAL SUPPLEMENT SERIES, 276:67 (14pp), 2025 February https://doi.org/10.3847/1538-4365/ada288

ExoMolHR: A Relational Database of Empirical High-resolution Molecular Spectra

Jingxin Zhang[1], Christian Hill[2], Jonathan Tennyson[1], and Sergei N. Yurchenko[1]
[1] Department of Physics and Astronomy, University College London, Gower Street, London WC1E 6BT, UK; jingxin.zhang.19@ucl.ac.uk
[2] International Atomic Energy Agency, Vienna A-1400, Austria
Received 2024 November 7; revised 2024 December 16; accepted 2024 December 19; published 2025 February 5

Abstract

ExoMolHR is an empirical, high-resolution molecular spectrum calculator for the high-temperature molecular line lists available from the ExoMol molecular database. Uncertainties, where available, in recommended ExoMol data sets are used to select highly accurate spectral lines. These lines largely rely on empirical energy levels generated through the MARVEL procedure, which is being systematically used to improve the energy and transition data provided by the ExoMol database. The freely accessible ExoMolHR database provides line positions with calculated intensities for a user-specified wavenumber/wavelength range and temperature. Spectra can be plotted on the ExoMolHR website https://www.exomol.com/exomolhr/ or downloaded as a .csv file. Cross sections can be calculated using the Python program PyExoCross. The ExoMolHR database currently provides 24,307,135 spectral lines for 33 molecules and 58 isotopologues; these numbers will increase as the ExoMol database is updated.

Unified Astronomy Thesaurus concepts: Molecular spectroscopy (2095)

1. Introduction

The assignment and analysis of astronomical spectra is generally performed using laboratory spectra. A number of spectroscopic databases are available to aid astronomers in this activity. Notable for long-wavelength studies are the Cologne Database for Molecular Spectroscopy (C. P. Endres et al. 2016) and the Jet Propulsion Laboratory submillimeter, millimeter, and microwave spectral-line catalog (H. M. Pickett et al. 1998) which have proved to be the mainstay of observational radio astronomy. Similarly, there are careful compilations of atomic spectra provided by sources such as the National Institute of Standards and Technology (NIST) Atomic Databases (A. Kramida et al. 2015; A. Kramida et al. 2020), R. L. Kurucz (2011), and the Vienna Atomic Line Database (T. Ryabchikova et al. 2015). For molecular spectra at shorter wavelengths the situation is less straightforward. The HITRAN (I. E. Gordon et al. 2022) database contains line data at largely infrared wavelengths for 55 molecules selected primarily for studies of the Earth's atmosphere at temperatures close to 296 K. Similarly the Gestion et Etude des Informations Spectroscopiques Atmosphériques (GEISA) database contains line data for 57 molecules which are substantially the same as those given by HITRAN. We note that the HITEMP project, while extending the temperature range of HITRAN data, only currently contains line lists for eight molecules (L. S. Rothman et al. 2010; R. J. Hargreaves et al. 2019), all of which feature in both HITRAN and GEISA.

J. Tennyson & S. N. Yurchenko (2012) started the ExoMol database to provide molecular line lists for exoplanet and other (hot) atmospheres. Originally the emphasis of this project has been on completeness of these line lists (S. N. Yurchenko et al. 2014) rather than accuracy. However, over the last few years we have increasingly used experimental data to improve the accuracy of line positions provided by the database, see L. K. McKemmish et al. (2024) for example. As a result the latest ExoMol data release (J. Tennyson et al. 2024b) claims 41 molecules for which high-accuracy transition wavenumbers are available for at least one isotopologue. The molecules considered in the ExoMol database are selected for their astronomical importance and data are provided for studies covering extended temperature ranges. The provision of high-accuracy data in ExoMol is an important step forward; however, the ExoMol database is huge, much larger than any of those quoted above, as it contains in the region of 10^{13} transitions. As described below, the high-accuracy lines given by ExoMol form only a small a proportion of the total, currently 24,307,135 transitions. The sheer volume of data in the ExoMol database makes it unsuitable for the sort of detailed spectroscopic analysis involved in, for example, initial line assignments. The aim of this work is to provide easy access to the high-resolution molecular data contained in the ExoMol database which can be used for assignment and analysis of strong lines.

ExoMol has been undertaking a systematic activity improving the accuracy of the energy levels, and hence transition frequencies, provided using the measured active rotation vibration energy levels (MARVEL) procedure (T. Furtenbacher et al. 2007; J. Tennyson et al. 2024a). A number of dedicated MARVEL studies have been performed recently on species such as C_2 (L. K. McKemmish et al. 2020), AlO (C. A. Bowesman et al. 2021), H_3^+ and its deuterated isotopologues (C. A. Bowesman et al. 2023), formaldehyde (A. R. Al-Derzi et al. 2021; M. Germann et al. 2024), methane (K. Kefala et al. 2024) and VO (C. A. Bowesman et al. 2022); recent work by L. K. McKemmish et al. (2024) has shown how MARVEL studies can be leveraged to extend the number of accurately determined energy levels and transitions. Accurate energy levels generated by MARVEL and related techniques are used by ExoMol to improve the accuracy of their data by replacing calculated energy levels with empirically determined ones. It is important to note that this technique usually leads to many more high-accuracy transitions being provided by ExoMolHR than have actually been observed in the laboratory, see

Table 1
Specification of the .states File including Extra Data Options

Field	Fortran Format	C Format	Description
i	I12	%12d	State ID
$\tilde{E}$	F12.6	%12.6f	Recommended state energy in cm^{-1}
g_{tot}	I6	%6d	Total state degeneracy
J	I7/F7.1	%7d/%7.1f	Total angular momentum quantum number, J or F (integer/half-integer)
Unc	F12.6	%12.6f	Uncertainty in the state energy in cm^{-1}
τ	ES12.4	%12.4E	State lifetime (aggregated radiative and predissociative lifetimes) in seconds
(g)	F10.6	%10.6f	Landé g-factor (optional)
(QN)	See .def file	See .def file	State quantum numbers, may be several columns (optional)
(Abbr)	A2	%2s	Abbreviation giving source of state energy (optional)
($\tilde{E}_0$)	F12.6	%12.6f	Calculated state energy in cm^{-1} (optional)

Note. The formats at the end of the table are for the compulsory section only (J. Tennyson et al. 2024b).

A. R. Al-Derzi et al. (2021) or C. A. Bowesman et al. (2022) for example.

2. The ExoMol Database

The ExoMolHR database stores largely empirical high-resolution spectral lines extracted from the ExoMol database. While line strength is not used in the extraction procedure, these lines are largely the stronger ones. Before introducing ExoMolHR we summarize the contents of the ExoMol database.

The ExoMol project was designed for interpreting spectra and modeling atmospheres of (hot) exoplanets, cool stars, brown dwarfs, and other hot astronomical objects by providing comprehensive lists of high-temperature molecular spectroscopic transitions (J. Tennyson et al. 2016, 2020). In practice, ExoMol data is also appropriate for nonastronomical applications such as combustion studies. The ExoMol database is accessible from the ExoMol website at https://www.exomol.com/. The current ExoMol database 2024 release provided spectroscopic data for 91 molecules and 224 isotopologues (J. Tennyson et al. 2024b). While the majority of these data sets (55 molecules) were generated in house by members of the ExoMol project, the ExoMol database also hosts data sets for 36 molecules generated either in house at University College London (UCL) for other reasons or externally. Many of these hosted data sets contain high-accuracy transition data for the systems concerned, for example the data sets from Bernath's MolLIST project (P. F. Bernath 2020) are based on laboratory high-resolution measurements. However, ExoMolHR requires explicit uncertainties to be present in the data to enable their inclusion. At present explicit uncertainties are only available for three external data sets generated by McKemmish's group from University of New South Wales, namely CN (A.-M. Syme & L. K. McKemmish 2021), ZrO (A. N. Perri et al. 2023) and NH (A. N. Perri & L. K. McKemmish 2024).

The ExoMol database has a well-defined data structure (J. Tennyson et al. 2013, 2024b). The ExoMol master file (exomol.json) points to a definition file for each line list with the version number given by the latest update date in the format YYYYMMDD. The ExoMol database provides both native format .def and JavaScript Object Notation (JSON; F. Pezoa et al. 2016) format .def.json (<ISOTOPOLOGUE>__<DATASET>.def.json) files which provide the information on molecular characteristics, uncertainty availability, quantum number labels and formats, and much else to allow for interpretation and automated processing the states and transitions. We used the information provided by these .def files to generate the ExoMolHR database.

Table 2
Specification of the .trans File including Extra Data Options

Field	Fortran Format	C Format	Description
f	I12	%12d	Upper-state ID
i	I12	%12d	Lower-state ID
A	ES10.4	%10.4E	Einstein A coefficient in s^{-1}
$\tilde{\nu}_{fi}$	E15.6	%15.6E	Transition wavenumber in cm^{-1} (optional)

Table 3
Specification of the .pf Partition Function File Format

Field	Fortran Format	C Format	Description
T	F8.1	%8.1f	Temperature in kelvin
$Q(T)$	F15.4	%15.4f	Partition function (dimensionless)

The ExoMol database is structured around two core file types: states (.states) and transitions (.trans) files (J. Tennyson et al. 2013). The .states files document the energy levels and their associated quantum numbers, while the .trans files store the Einstein A coefficients identified by upper- and lower-state indices that reference the corresponding entries in the .states files. Due to their potentially large size, especially the .trans files, both types of files are compressed using the .bz2 format. For some large line lists, the transitions are divided into multiple files in a series, each covering a specific wavenumber region as indicated in the file name. Partition function (.pf) files provided by the ExoMol database are also used by the ExoMolHR database to calculate transition intensities. Tables 1, 2, and 3 illustrate the structure of the .states, .trans, and .pf files, respectively. Note that the uncertainty column, labeled "Unc" in Table 1, is a relatively new feature in the ExoMol database and not all data sets contain uncertainties. ExoMolHR requires the uncertainties to be present so that data sets without an Unc column (as determined from the ExoMol .def.json file) are simply ignored. However, these data sets are substantially ones that have not been updated using MARVEL energy levels which therefore do not contain any high-accuracy data of interest for ExoMolHR.

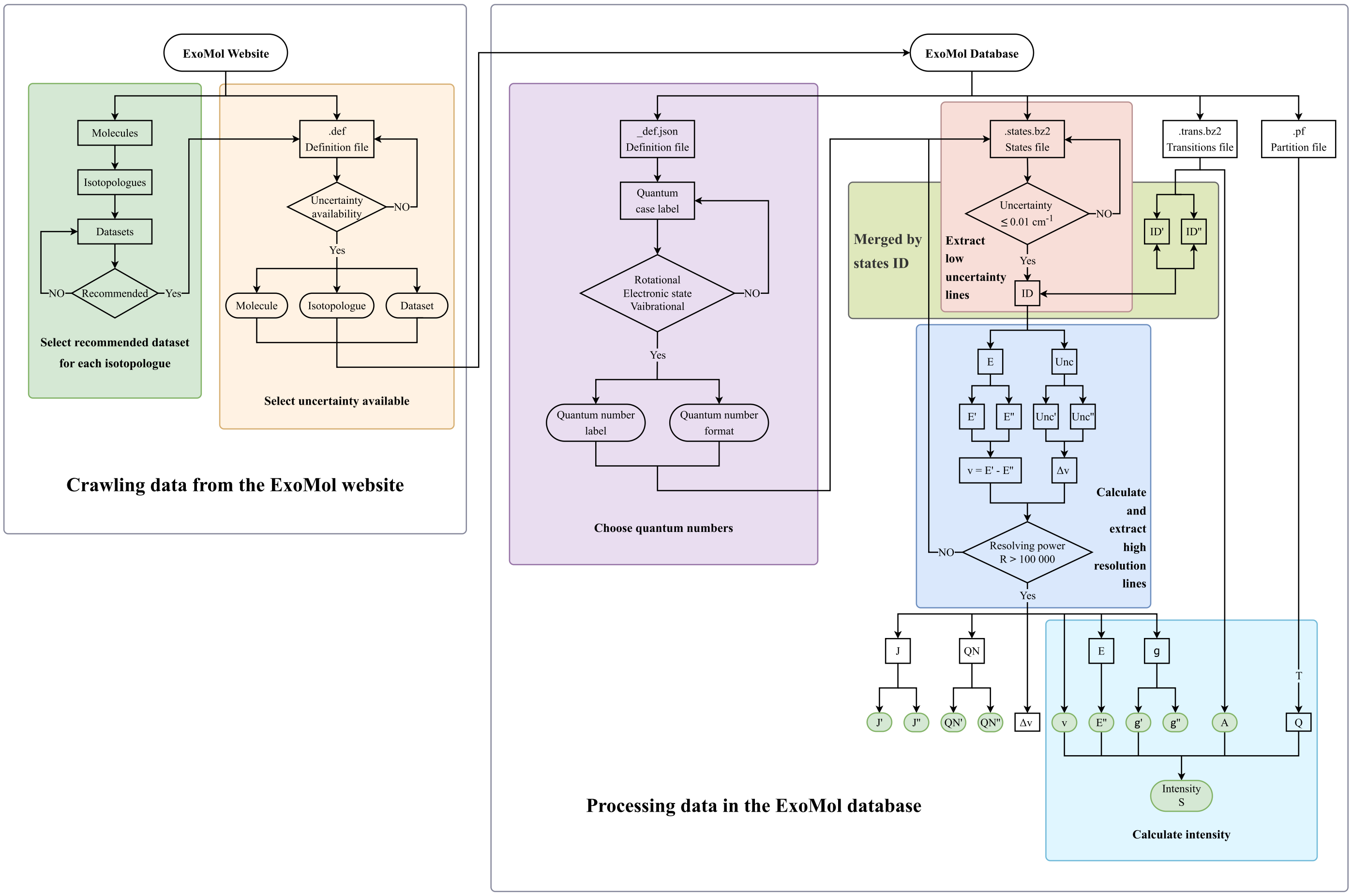

Figure 1. Process flowchart for ExoMolHR database generation.

Table 4
Specification of the Output .csv ExoMolHR File Format

Field	Fortran Format	C Format	Description
$\tilde{\nu}$ or $\tilde{\lambda}$	F12.6	%12.6f	Transition wavenumber/frequency in cm^{-1} or wavelength in micrometers
Unc	F12.6	%12.6f	Uncertainty in the state energy in cm^{-1}
A	ES10.4	%10.4E	Einstein A coefficient in s^{-1}
S	ES10.4	%10.4E	Absorption intensity at the user-specified temperature in centimeters per molecule
E''	F12.6	%12.6f	Lower-state energy in cm^{-1}
g'	I6	%6d	Total state degeneracy for upper state
g''	I6	%6d	Total state degeneracy for lower state
J'	I7/F7.1	%7d/%7.1f	Total angular momentum quantum number (integer/half-integer) for upper state
J''	I7/F7.1	%7d/%7.1f	Total angular momentum quantum number (integer/half-integer) for lower state
(QN$'$)	See .def file	See .def file	Quantum number for upper state (optional)
(QN$''$)	See .def file	See .def file	Quantum number for lower state (optional)

Note. Quantum number labels and formats are defined in the ExoMol definition file, .def.json.

3. Methodology and Algorithm

The ExoMolHR database is designed to provide highly accurate line positions for high-resolution studies, such as identifying spectral lines or simulating high-resolution spectra. Figure 1 illustrates how the ExoMolHR database is generated. This process requires data to be obtained separately from the ExoMol websites and its database by following steps. Initially, we scraped data from the ExoMol website for all molecules and isotopologues. We extract the recommended data set for each isotopologue and then iterate through their definition file (.def.json), processing only those data sets for which explicit uncertainties are available. Next, we process the line list files to obtain the labels and formats of the quantum numbers from the ExoMol JSON format definition files (.def.json) and keep only ;the vibrational, rotational, and electronic-state quantum numbers in the .states files. Subsequently, we extract those lines from the .states and .trans files of the ExoMol database which are determined to high accuracy (low uncertainty); in practice energy levels with

Table 5
Extract from the ExoMolHR File of $^{1}H_2^{16}O$ at Temperature $T = 296$ K (`yyyymmddhhmmss__1H2-16O__296.0K.csv`)

$\tilde{\nu}$	Unc.	A	S	$\tilde{E}''$	g'	g''	J'	J''	Γ'	v'_1	v'_2	v'_3	K'_a	K'_c	$\Gamma''_{\rm rve}$	v''_1	v''_2	v''_3	K''_a	K''_c
500.018142	0.000029	2.3792E–03	1.3746E–30	4195.818039	15	13	7	6	A2	1	0	0	5	3	A1	0	0	1	1	6
500.035515	0.000009	1.7621E–01	2.3697E–24	2248.063135	27	27	13	13	A1	0	0	0	6	8	A2	0	0	0	3	11
500.436638	0.000023	3.8196E–04	1.3245E–30	4052.836634	45	45	7	7	B1	0	0	1	3	5	B2	0	2	0	3	4
500.621556	0.000028	9.2079E–02	3.4260E–23	1774.750359	75	75	12	12	B2	0	0	0	5	8	B1	0	0	0	2	11
500.661272	0.000012	2.6278E–04	2.3620E–30	4006.071011	93	99	15	16	B1	0	1	0	2	13	B2	0	0	0	7	10
500.878899	0.000050	1.9196E–01	1.0828E–24	2426.195175	27	27	13	13	A2	0	0	0	7	7	A1	0	0	0	4	10
501.573101	0.000071	5.8196E+01	2.2409E–22	2471.254912	23	21	11	10	A1	0	0	0	10	2	A2	0	0	0	9	1
501.573504	0.000071	5.8196E+01	6.7226E–22	2471.254532	69	63	11	10	B1	0	0	0	10	1	B2	0	0	0	9	2
502.064969	0.000043	6.5476E–03	2.4083E–30	4257.786653	13	11	6	5	A2	0	0	1	6	1	A1	1	0	0	4	2

Notes. yyyymmddhhmmss: the file name is structured with 14 digits of created date and time, iso-slug, and temperature. yyyymmdd means date with year, month, and day. hhmmss means time with hour, minute, and second; $\tilde{\nu}$: transition wavenumber/frequency in cm^{-1}; Unc: uncertainty in the transition wavenumber in cm^{-1}; A: Einstein A coefficient in s^{-1}; S: absorption intensity in centimeters per molecule; $\tilde{E}''$: lower-state energy in cm^{-1}; g' and g'': total state degeneracy for upper and lower state; J' and J'': total angular momentum rotational quantum number for upper and lower state, excluding nuclear spin; Γ' and Γ'': rovibrational symmetry label for upper and lower state; v'_1 and v''_1: v_1 symmetric stretch quantum number for upper and lower state; v'_2 and v''_2: v_2 bend quantum number for upper and lower state; v'_3 and v''_3: v_3 asymmetric stretch quantum number for upper and lower state; K'_a and K''_a: K_a rotational quantum number for upper and lower state; K'_c and K''_c: K_c rotational quantum number for upper and lower state.

Table 6
Quantum Number Labels for Each Isotopologue in the ExoMolHR Database

Molecule	Isotopologue	Quantum Number Label
AlCl	^{27}Al^{35}Cl, ^{27}Al^{37}Cl	+/− e/f ElecState v Λ Σ Ω
AlH	^{27}Al^{1}H	...
AlO	^{26}Al^{16}O, ^{27}Al^{16}O, ^{27}Al^{17}O, ^{27}Al^{18}O	...
BeH	^{9}Be^{1}H, ^{9}Be^{2}H	...
C_2	$^{12}C_2$	...
CaH	^{40}Ca^{1}H	...
CN	^{12}C^{14}N	...
MgH	^{24}Mg^{1}H, ^{25}Mg^{1}H, ^{26}Mg^{1}H	...
NO	^{14}N^{16}O	...
PN	^{31}P^{14}N	...
SiN	^{28}Si^{14}N, ^{28}Si^{15}N, ^{29}Si^{14}N, ^{30}Si^{14}N	...
SiO	^{28}Si^{16}O	...
TiO	^{47}Ti^{16}O	...
VO	^{51}V^{16}O	...
YO	^{89}Y^{16}O, ^{89}Y^{17}O, ^{89}Y^{18}O	...
ZrO	^{90}Zr^{16}O, ^{91}Zr^{16}O, ^{92}Zr^{16}O, ^{93}Zr^{16}O, ^{94}Zr^{16}O, ^{96}Zr^{16}O	...
SO	^{32}S^{16}O	+/− ElecState v Λ Σ Ω
LiOH	^{6}Li^{16}O^{1}H, ^{7}Li^{16}O^{1}H	+/− e/f ElecState v_1 v_2 l_2 v_3
NH	^{14}N^{1}H, ^{14}N^{2}H, ^{15}N^{1}H, ^{15}N^{2}H	+/− e/f ElecState v Λ N F
CaOH	^{40}Ca^{16}O^{1}H	+/− e/f N ElecState L v_1 v_2 l_2 v_3 Ω F1/F2/F3
SO_2	$^{32}S^{16}O_2$	+/− K_a K_c v_1 v_2 v_3
H_2O	$^{1}H_2^{16}O$	$G_{\rm rve}$ v_1 v_2 v_3 K_a K_c
H_2S	$^{1}H_2^{32}S$	...
H_3^+	$^{1}H_3^+$, $^{2}H_3^+$	e/f $G_{\rm rve}$ N Isomer v_1 v_2 l_2 G U K
	$^{1}H_2^{2}H^+$, $^{2}H_2^{1}H^+$	+/− $G_{\rm rve}$ N Isomer v_1 v_2 v_3 K_a K_c
NH_3	$^{14}N^{1}H_3$	+/− $G_{\rm tot}$ N n_1 n_2 n_3 n_4 l_3 l_4 τ_i K $G_{\rm rot}$
	$^{15}N^{1}H_3$	$G_{\rm tot}$ n_1 n_2 n_3 l_3 n_4 l_4 $G_{\rm vib}$ K $G_{\rm rot}$
C_2H_2	$^{12}C_2^{1}H_2$	$G_{\rm tot}$ K e/f $G_{\rm rot}$
N_2O	$^{14}N_2^{16}O$	$G_{\rm tot}$ n_1 $n_2 lin$ l_2 n_3 P N
H_3O^+	$^{1}H_3^{16}O^+$	$G_{\rm tot}$ n_1 n_2 n_3 l_3 n_4 l_4 K $G_{\rm rot}$
CH_4	$^{12}C^{1}H_4$	$G_{\rm tot}$ n_1 n_2 l_2 n_3 l_3 M_3 n_4 l_4 M_4 n
CO_2	$^{12}C^{16}O_2$	$G_{\rm tot}$ e/f n_1 n_2 l_2 n_3 m_1 m_2 m_3 m_4 m_5
H_2CO	$^{1}H_2^{12}C^{16}O$	$G_{\rm tot}$ v_1 v_2 v_3 v_4 v_5 v_6 K_a K_c
H_2CS	$^{1}H_2^{12}C^{32}S$	$G_{\rm tot}$ v_1 v_2 v_3 v_4 v_5 v_6 K_a K_c
OCS	$^{16}O^{12}C^{32}S$	$G_{\rm tot}$ v_1 v_2 l_2 v_3 e/f $G_{\rm vib}$ $G_{\rm rot}$ Coef n_1 n_2 n_3

Note. Electronic-state term values are defined using PYVALEM format (C. Hill & M. Hanicinec 2022; C. Hill et al. 2025, in preparation).

an uncertainty $\Delta E \leqslant 0.01$ cm^{-1} in the `.states` file are retained for processing into transition wavenumbers.

Resolving power, R, is defined by the wavelength λ and its uncertainty $\Delta\lambda$. Here we use the transition wavenumber $\tilde{\nu}$ and its uncertainty $\Delta\tilde{\nu}$ to calculate the resolving power R as

$$R = \frac{\lambda}{\Delta\lambda} \approx \frac{\tilde{\nu}}{\Delta\tilde{\nu}}, \tag{1}$$

where the transition wavenumber (frequency) $\tilde{\nu}$ is equal to the upper-state energy $\tilde{E}'$ minus the lower-state energy $\tilde{E}''$:

$$\tilde{\nu} = \tilde{E}' - \tilde{E}'', \tag{2}$$

and

$$\Delta\tilde{\nu} = \sqrt{(\Delta E')^2 + (\Delta E'')^2}. \tag{3}$$

$\Delta E'$ and $\Delta E''$ are the uncertainties of the upper- and lower-state energy levels, respectively. Finally, we scrape high-resolution transitions which are determined to correspond to $R > 100{,}000$. The ExoMolHR database supports calculating absorption line intensities I_{fi} (cm molecule^{-1}) at different temperatures T in kelvin provided by users with Equation (4) (U. G. Jørgensen et al. 1996; S. N. Yurchenko et al. 2018):

$$I_{f\leftarrow i} = \frac{g'_f A_{fi}}{8\pi c \tilde{\nu}_{fi}^2} \frac{e^{-c_2 \tilde{E}''_i/T}(1 - e^{-c_2\tilde{\nu}_{fi}/T})}{Q(T)}. \tag{4}$$

g'_f is the upper-state degeneracy and $\tilde{E}''_i$ is the lower-state energy in the `.states` file. A_{fi} is the Einstein A coefficient (s^{-1}) in the `.trans` file. $\tilde{\nu}_{fi}$ is the transition wavenumber (cm^{-1}) in the `.trans` file for small data sets or calculated by Equation (2). $c_2 = hc/k_B$ is the second radiation constant (centimeter kelvin), where h is the Planck constant (erg second), c is the speed of light (cm s^{-1}), and k_B is the Boltzmann constant (erg K^{-1}). $Q(T)$ is the temperature-dependent partition function given by the ExoMol partition function file (`.pf`).

4. ExoMolHR Database Overview

ExoMolHR is an extensive high-resolution molecular spectroscopic database based on the ExoMol database which contains molecular line lists designed for studies of hot environments. ExoMolHR database is hosted at https://www.exomol.com/exomolhr/. This is initial offering contains lines for 58 isotopologues associated with 33 molecules that are supported on the ExoMolHR website, see Table 8 below.

This section will introduce the file structure and features (Section 4.1), use cases (Section 4.2), the application programming interface (API; Section 4.3), and a summary of line lists in the ExoMolHR database.

4.1. File Structure and Features

Table 4 specifies the ExoMolHR database file structure and Table 5 is a sample of the ExoMolHR database file (`.csv`) for $^{1}H_2^{16}O$ at temperature $T = 296$ K. Transitions form the core of the ExoMolHR database including the frequency (which can be extracted for a user-specified wavenumber range), transition uncertainty, Einstein A coefficient, intensity (at a user-specified temperature), lower-state energy level, total degeneracy, angular momentum, and quantum numbers for upper and lower states. The output `.csv` are not provided on the website but their contents (with an extra intensity column for the user-specified temperature) can be extracted simply by requesting data for the given wavenumber or wavelength range for the species of interest.

ExoMol state files, particularly those for polyatomic molecules, often have multiple sets of quantum numbers. However, for simplicity, the ExoMolHR database only provides a single set of quantum numbers for each state which are generally based on a standard, normal-mode description of the vibrational motion. If needed, the alternative quantum number descriptions can be obtained from the appropriate `.states` file.

Table 7
The Formats and Descriptions Corresponding to Quantum Number Labels

Label	Fortran Format	C Format	Description
J	I7/F7.1	%7d/%7.1f	Total angular momentum
	I7	%7d	AlCl, AlH, C_2, C_2H_2, CH_4, CO_2, H_2CO, H_2CS, H_2O, H_2S, H_3^+, H_3O^+, LiOH, N_2O, NH, NH_3, OCS, PN, SiO, SO, SO_2, TiO, VO
	F7.1	%7.1f	AlO, BeH, CN, CaH, CaOH, MgH, NO, SiN, YO, ZrO
+/−	A1	%1s	Total parity
e/f	A1	%1s	Rotationless parity
ElecState	A12	%12s	Electronic-term value
v	I3	%3d	Vibrational quantum number
$\|\Lambda\|$	I3	%3d	Absolute value of the projection of electronic angular momentum
$\|\Sigma\|$	I3	%3d	Absolute value of the projection of the electronic spin
$\|\Omega\|$	I5/F5.1	%5d/%5.1f	Absolute value of the projection of the total angular momentum
	I5	%5d	AlCl, AlH, C_2, TiO, ZrO
	F5.1	%5.1f	AlO, BeH, CN, CaH, CaOH, MgH, NO, PN, SO, SiN, SiO, VO, YO
G_{tot}	A3	%3s	Total symmetry
G_{rot}	A3	%3s	Symmetry of rotational contribution
G_{rve}	A3	%3s	Rovibrational symmetry label for upper and lower state
G_{vib}	A3	%3s	Symmetry of vibrational contribution
N	I5	%5d	Vibrational state ID or rotational angular momentum
L	I3	%3d	Vibronic angular momentum quantum number
P	I2	%2d	Polyad number
F	I2	%2d	Fine structure counting number
F1/F2/F3	I2	%2d	Spin components F1 and F3
U	A1	%1s	U-notation of J. K. G. Watson (1984)
G	I2	%2d	Absolute value of $k - l_2$
K	I2	%2d	State projection of the J. K. G. Watson (1984) rotational quantum number
K_a	I2	%2d	K_a rotational quantum number
K_c	I2	%2d	K_c rotational quantum number
M_3, M_4	I2	%2d	Multiplicity index quantum numbers
v_1, v_2, v_3, v_4, v_5, v_6	I2	%2d	v_i local-mode vibrational quantum numbers
l_2, l_3, l_4	I2	%2d	Normal-mode vibrational angular momentum quantum number
n_1, n_2, n_3, n_4	I2	%2d	Normal-mode vibrational quantum numbers
m_1, m_2, m_3, m_4, m_5	I2	%2d	HITRAN normal-mode quantum number I. E. Gordon et al. (2022)
n	I2	%2d	Polyad or rotational counting number
n_2lin	I2	%2d	Normal-mode linear molecule bending quantum number
τ_i	I1	%1d	Inversion parity (0 or 1)
Isomer	A1	%1s	Nuclear spin isomer
Coef	F5.2	%5.2f	Coefficient with the largest contribution to the ($J = 0$) contracted set

Note. Electronic-state term values are defined using PYVALEM format (C. Hill & M. Hanicinec 2022; C. Hill et al. 2025, in preparation). The descriptions of the labels in the table are for reference only. Sometimes there may be slight variations in their usage. More accurate and detailed descriptions are available in the definition file, `.def.json`, for the recommended data set for each isotopologue. The meaning of each label can be further understood by referring to the notes under the example tables in the corresponding line list papers.

The ExoMolHR files are named in the format `<yyyymmddhhmmss>__<ISO-SLUG>__<T>K.csv` where `<yyyymmddhhmmss>` is a 14-digit character string corresponding to a time stamp in the format of year (`yyyy`), month (`mm`), day (`dd`), hour (`hh`), minute (`mm`), and second (`ss`). `<T>` is the temperature rounded to one decimal place in kelvin. The ExoMolHR database calculates the intensity at specified temperatures and is filtered by wavenumber range and minimal intensity. The downloaded data is provided in `.csv` format and uses the column names given in Table 4 as the header.

Table 6 displays the quantum number labels and the format of the quantum number J for each isotopologue in the ExoMolHR database. Table 7 details the formats and descriptions of quantum numbers for various quantum number labels. The electronic-state term values in both ExoMol and ExoMolHR databases are defined using PyValem format. PyValem (C. Hill & M. Hanicinec 2022; C. Hill et al. 2025, in preparation) is a Python package designed for parsing, validating, manipulating, and interpreting chemical formulas, quantum states, and labels of atoms, ions, and small molecules. For example, $X^1\,\Sigma^+$ is written as `X`(1SIGMA+). Sometimes, due to conventional differences in the notation used for the quantum number labels of different molecules in the ExoMol definition files (`.def`), there are differences in the notation adopted between molecules meaning that v_i, n_i, or m_i can represent similar quantum numbers.

4.2. Use Cases

The ExoMolHR website provides a download link to the `.csv` file(s) that contain the calculated results, and plots the stick spectra for one or multiple isotopologues. Users can use the following steps to obtain the final results. Figure 2 shows the screenshots of these four steps.

Step 1. Molecules: Users can choose one or multiple molecules from the form. There are two search boxes for searching by molecule name and formula.

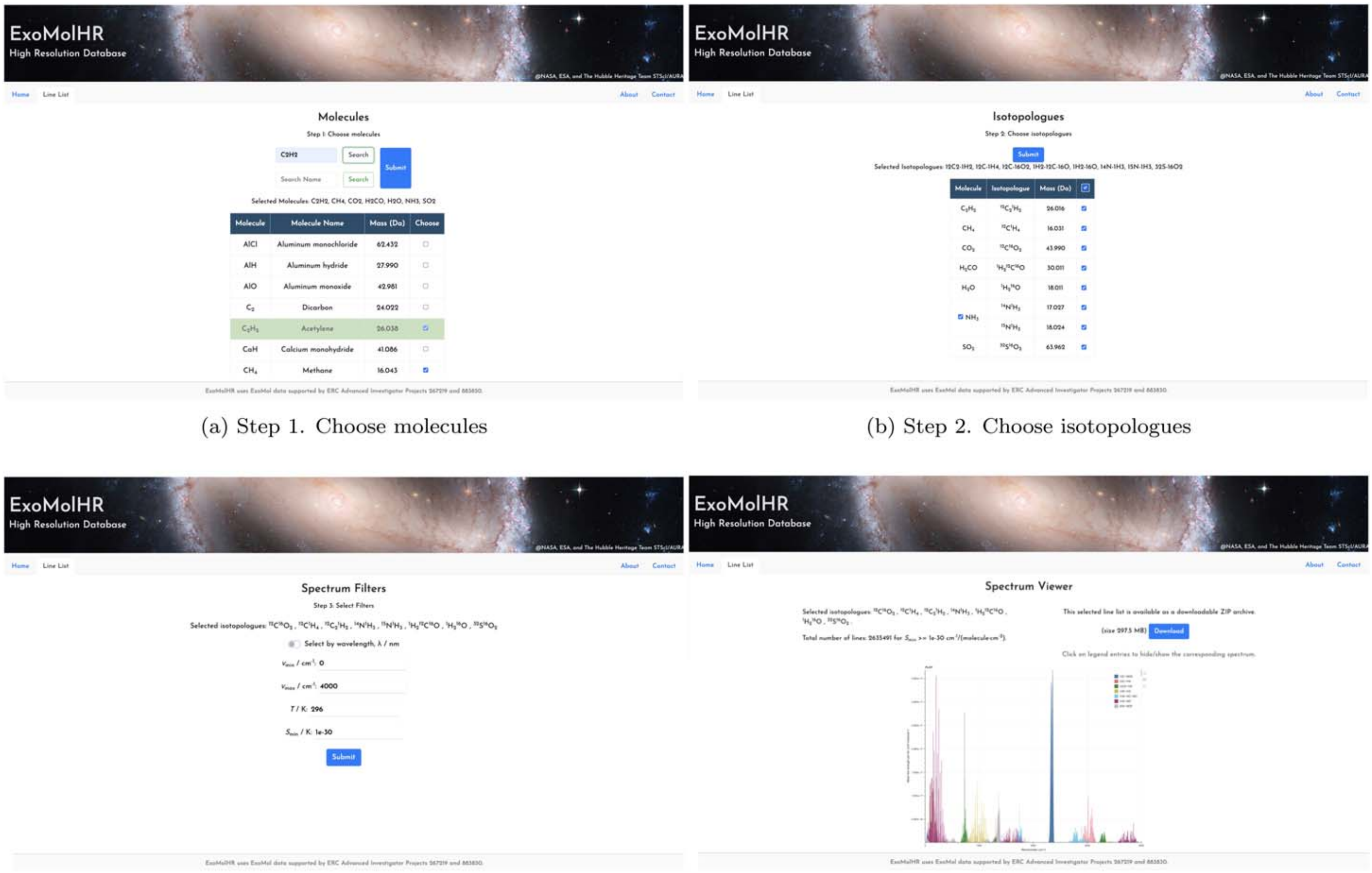

(a) Step 1. Choose molecules

(b) Step 2. Choose isotopologues

(c) Step 3. Select filters

(d) Step 4. Spectrum viewer

Figure 2. Four steps for getting the intensity file from the ExoMolHR website.

Step 2. Isotopologues: similarly, one or more isotopologues can be selected in this step; users can select all isotopologues by clicking the "select all" button.

Step 3. Spectral filters: users can define the wavenumber range by the given ν_{min} and ν_{max} in cm^{-1} or wavelength range by λ_{min} and λ_{max} in micrometers, temperature T in kelvin, and minimum intensity S_{min} in cm $molecule^{-1}$.

Step 4. Spectrum viewer: finally, users are provided with a plot of intensities calculated at the given temperature for one or multiple isotopologues in different colors for the requested wavenumber range. The web page also provides the number of lines and file size for total result files. Users can download a compressed `.zip` file and the result files are named separately for each species/isotopologues. The structure of this file is specified in Section 4.1.

Note the ExoMolHR website only plots stick spectra. The ExoMol database provides a set of pressure-broadening parameters (E. J. Barton et al. 2017; E. R. Guest et al. 2024; J. Buldyreva et al. 2025). These parameters can be combined with the `.csv` file to provide temperature and pressure-dependent cross sections. The python program PyExoCross (J. Zhang et al. 2024) is being adapted to ingest the intensities from the ExoMolHR database and the broadening parameters from the ExoMol database to calculate the cross sections. However, we note that for most problems this process should probably use the original ExoMol line list to ensure the inclusion of all lines in the spectral region of interest.

4.3. Application Programming Interface

Users can use the API to jump to the spectrum viewer website. The API format is https://www.exomol.com/exomolhr/get-data/?numin=<ν_{min}>&numax=<ν_{max}>&T=<T>&Smin=<S_{min}>&iso=<ISO-SLUG$_i$>. If multiple isotopologues are requested, then &iso=<ISO-SLUG$_i$> should be used repeatedly to specify these different isotopologues. For example, &iso=<ISO-SLUG$_1$>&iso=<ISO-SLUG$_2$>. As an example, a user request for ExoMolHR files with intensities calculated at temperature $T = 296$ K with an intensity threshold for $S_{min} = 10^{-30}$ cm $molecule^{-1}$ for $^{1}H_2^{16}O$, $^{12}C^{16}O_2$, and $^{32}S^{16}O_2$ in the wavenumber range from $\nu_{min} = 0$ to $\nu_{max} = 1000$ cm^{-1} has the API https://www.exomol.com/exomolhr/get-data/?numin=450&numax=600&T=296&Smin=1e-21&iso=1H2-16O&iso=12C-1H4&iso=32S-16O2. Note that in the file name the species are ordered in the order of the original request.

The ExoMolHR compressed `.zip` file is named with the creation date and time, which has 14 digits in the format yyyymmddhhmmss (year, month, day, hour, minute, and second), for example, https://www.exomol.com/exomolhr/get-data/download/?archive_name=20240907222904.zip. This means users cannot directly download files via the API, but they can still be downloaded by clicking the download button on the spectrum viewer website. This method is typically more intuitive and ensures that users can see the data visualization and file details they are about to download before

Table 8
Summary of Lines with Low Uncertainties and High Resolutions Extracted from the ExoMol Database and Used to Form the ExoMolHR Database

ID_m	Molecule	ID_i	Isotopologue	Data Set	Version	N_{states}	N_{files}	N_{trans}	$Size_{trans}$	$N_{HRstates}$	$N_{HRlines}$	$Size_{HR}$	ExoMol Line List
1	AlCl	1	$^{27}Al^{35}Cl$	YNAT	20221231	65,869	1	4,722,048	47.5 MB	41	101	15.3 KB	S. N. Yurchenko et al. (2023)
		2	$^{27}Al^{37}Cl$	YNAT	20221231	67,507	1	5,748,704	57.7 MB	41	121	18.4 KB	⋯
2	AlH	3	$^{27}Al^1H$	AloHa	20240307	1364	1	29,725	152.9 KB	135	692	104.2 KB	S. N. Yurchenko et al. (2024e)
3	AlO	4	$^{26}Al^{16}O$	ATP	20210622	93,350	1	4,866,540	53.6 MB	4783	143,197	21.0 MB	C. A. Bowesman et al. (2021)
		5	$^{27}Al^{16}O$	ATP	20210622	94,862	1	4,945,580	31.1 MB	4980	149,577	22.0 MB	⋯
		6	$^{27}Al^{17}O$	ATP	20210622	96,350	1	5,148,996	56.7 MB	4787	142,905	21.0 MB	⋯
		7	$^{27}Al^{18}O$	ATP	20210622	98,269	1	5,365,592	59.1 MB	4799	142,976	21.0 MB	⋯
4	BeH	8	$^9Be^1H$	Darby-Lewis	20240710	14,950	1	592,308	6.1 MB	132	507	76.4 KB	D. Darby-Lewis et al. (2020)
		9	$^9Be^2H$	Darby-Lewis	20240710	14,950	1	689,466	7.2 MB	104	310	46.8 KB	⋯
5	C_2	10	$^{12}C_2$	8states	20200628	44,189	1	6,080,920	68.7 MB	8376	445,682	65.5 MB	L. K. McKemmish et al. (2020)
6	C_2H_2	11	$^{12}C_2^1H_2$	aCeTY	20220918	5,160,803	100	4,347,381,911	96.1 GB	8898	473,850	47.9 MB	K. L. Chubb et al. (2020)
7	CH_4	12	$^{12}C^1H_4$	MM	20240113	9,155,208	121	50,395,644,806	439.0 GB	21,021	7,649,736	760.2 MB	S. N. Yurchenko et al. (2024d)
8	CN	13	$^{12}C^{14}N$	Trihybrid	20210526	28,004	1	2,285,103	25.8 MB	4833	244,808	36.0 MB	A.-M. Syme & L. K. McKemmish (2021)
9	CO_2	14	$^{12}C^{16}O_2$	UCL-4000	20200630	3,480‘477	20	2,557,549,946	21.7 GB	18,881	2,600,218	362.0 MB	S. N. Yurchenko et al. (2020a)
10	CaH	15	$^{40}Ca^1H$	XAB	20220211	6825	1	293,151	2.3 MB	1165	12,341	1.8 MB	A. Owens et al. (2022a)
11	CaOH	16	$^{40}Ca^{16}O^1H$	OYT6	20230523	3,187,522	18	23,384,729,495	202.0 GB	1424	12,984	1.6 MB	A. Owens et al. (2022b)
12	H_2CO	17	$^1H_2^{12}C^{16}O$	AYTY	20230430	10,297,025	100	12,688,112,669	111.1 GB	4813	317,729	41.2 MB	A. F. Al-Refaie et al. (2015)
13	H_2CS	18	$^1H_2^{12}C^{32}S$	MOTY	20221231	52,292,454	8	43,561,116,660	399.5 GB	3625	72,218	6.6 MB	T. Mellor et al. (2022)
14	H_2O	19	$^1H_2^{16}O$	POKAZATEL	20230621	810,269	412	5,745,071,340	48.1 GB	14,395	3,520,554	396.2 MB	O. L. Polyansky et al. (2018)
15	H_2S	20	$^1H_2^{32}S$	AYT2	20220918	220,631	35	115,032,941	873.0 MB	7314	1,084,520	122.0 MB	A. A. A. Azzam et al. (2016)
16	H_3O^+	21	$^1H_3^{16}O^+$	eXeL	20200707	1,173,114	100	2,089,331,073	10.1 GB	232	1785	251.3 KB	S. N. Yurchenko et al. (2020b)
17	H_3^+	22	$^1H_2^2H^+$	ST	20230123	33,330	1	22,164,810	128.2 MB	109	646	87.2 KB	C. A. Bowesman et al. (2023)
		23	$^1H_3^+$	MiZATeP	20230123	158,721	1	127,542,657	1.7 GB	994	13,606	1.9 MB	⋯
		24	$^2H_2^1H^+$	MiZo	20221221	369,500	32	2,290,235,000	14.8 GB	115	683	92.2 KB	⋯
		25	$^2H_3^+$	MiZo	20230124	37,410	21	36,078,183	170.3 MB	115	225	32.0 KB	⋯
18	LiOH	26	$^6Li^{16}O^1H$	OYT7	20231001	192,412	5	294,573,305	2.3 GB	255	840	113.3 KB	A. Owens et al. (2024a)
		27	$^7Li^{16}O^1H$	OYT7	20230529	203,762	5	331,274,717	2.6 GB	240	749	101.1 KB	⋯
19	MgH	28	$^{24}Mg^1H$	XAB	20220211	3148	1	88,575	953.2 KB	237	2462	370.4 KB	A. Owens et al. (2022a)
		29	$^{25}Mg^1H$	XAB	20220211	3156	1	88,776	955.6 KB	548	5850	879.9 KB	⋯
		30	$^{26}Mg^1H$	XAB	20220211	3160	1	88,891	956.5 KB	537	5339	803.1 KB	⋯
20	N_2O	31	$^{14}N_2^{16}O$	TYM	20240527	1,759,068	11	1,360,351,722	11.0 GB	17,018	3,459,640	309.9 MB	S. N. Yurchenko et al. (2024c)
21	NH	32	$^{14}N^1H$	kNigHt	20240301	4076	1	327,014	1.6 MB	1030	26,131	3.7 MB	A. N. Perri & L. K. McKemmish (2024)
		33	$^{14}N^2H$	kNigHt	20240301	7406	1	778,105	3.7 MB	118	943	136.4 KB	⋯
		34	$^{15}N^1H$	kNigHt	20240301	4089	1	327,877	1.6 MB	118	943	136.4 KB	⋯
		35	$^{15}N^2H$	kNigHt	20240301	7465	1	785,940	3.8 MB	118	943	136.4 KB	⋯
22	NH_3	36	$^{14}N^1H_3$	CoYuTe	20200730	5,095,730	200	16,941,637,250	142.9 GB	4720	412,149	64.4 MB	P. A. Coles et al. (2019)
		37	$^{15}N^1H_3$	CoYuTe-15	20240808	12,699,617	10	929,795,249	7.3 GB	2699	148,651	22.0 MB	S. N. Yurchenko et al. (2024a)
23	NO	38	$^{14}N^{16}O$	XABC	20210422	30,811	1	4,596,666	96.7 MB	3044	106,711	15.7 MB	Q. Qu et al. (2021)
24	OCS	39	$^{16}O^{12}C^{32}S$	OYT8	20240425	2,399,110	10	2,527,364,150	26.4 GB	5198	279,273	44.7 MB	A. Owens et al. (2024b)
25	PN	40	$^{31}P^{14}N$	PaiN	20240505	30,327	1	1,333,445	15.6 MB	32	44	6.8 KB	M. Semenov et al. (2025)
26	SO	41	$^{32}S^{16}O$	SOLIS	20230914	84,114	1	7,086,100	81.6 MB	536	2501	366.5 KB	R. P. Brady et al. (2024)
27	SO_2	42	$^{32}S^{16}O_2$	ExoAmes	20170131	3,270,271	80	1,300,000,000	25.4 GB	14,924	1,504,495	163.6 MB	D. S. Underwood et al. (2016)
28	SiN	43	$^{28}Si^{14}N$	SiNfull	20220809	131,936	1	43,646,806	506.9 MB	99	670	100.9 KB	M. Semenov et al. (2022)
		44	$^{28}Si^{15}N$	SiNfull	20220809	133,460	1	44,816,182	520.9 MB	56	464	69.9 KB	⋯
		45	$^{29}Si^{14}N$	SiNfull	20220809	132,335	1	43,946,969	510.6 MB	56	464	69.9 KB	⋯
		46	$^{30}Si^{14}N$	SiNfull	20220809	132,706	1	44,223,730	513.9 MB	56	464	69.9 KB	⋯
29	SiO	47	$^{28}Si^{16}O$	SiOUVenIR	20211105	174,250	1	91,395,763	1.1 GB	911	8729	1.3 MB	S. N. Yurchenko et al. (2022)
30	TiO	48	$^{48}Ti^{16}O$	Toto	20210825	301,245	1	58,983,952	689.5 MB	8725	499,775	73.4 MB	L. K. McKemmish et al. (2019)

Table 8
(Continued)

ID_m	Molecule	ID_i	Isotopologue	Data Set	Version	N_{states}	N_{files}	N_{trans}	$Size_{trans}$	$N_{HRstates}$	$N_{HRlines}$	$Size_{HR}$	ExoMol Line List
31	VO	49	$^{51}V^{16}O$	HyVO	20231218	3,410,598	90	58,904,173,243	297.9 GB	7043	635,722	68.1 MB	C. A. Bowesman et al. (2024)
32	YO	50	$^{89}Y^{16}O$	BRYTS	20230916	173,621	1	60,678,140	719.1 MB	28	25	3.9 KB	S. N. Yurchenko et al. (2024b)
		51	$^{89}Y^{17}O$	BRYTS	20230916	182,598	1	62,448,157	740.9 MB	28	25	3.9 KB	⋯
		52	$^{89}Y^{18}O$	BRYTS	20230916	182,547	1	64,164,605	761.9 MB	28	25	3.9 KB	⋯
33	ZrO	53	$^{90}Zr^{16}O$	ZorrO	20230713	227,118	1	47,662,773	369.3 MB	5313	145,317	21.3 MB	A. N. Perri et al. (2023)
		54	$^{91}Zr^{16}O$	ZorrO	20230713	227,118	1	47,748,501	370.1 MB	1058	5164	776.8 KB	⋯
		55	$^{92}Zr^{16}O$	ZorrO	20230713	227,124	1	47,830,250	370.8 MB	1058	5164	776.8 KB	⋯
		56	$^{93}Zr^{16}O$	ZorrO	20230713	227,126	1	47,928,979	371.6 MB	1058	5164	776.8 KB	⋯
		57	$^{94}Zr^{16}O$	ZorrO	20230713	227,128	1	47,994,352	372.1 MB	1058	5164	776.8 KB	⋯
		58	$^{96}Zr^{16}O$	ZorrO	20230713	227,134	1	48,136,388	373.3 MB	1058	5164	776.8 KB	⋯

Notes. ID_m: molecule index; ID_i: isotopologue index; Version: ExoMol data set update date in the format YYYYMMDD; N_{states}: number of states in states file; N_{files}: number of transitions files; N_{trans}: number of transitions in transitions file(s); $Size_{trans}$: total file size of bzip2 compressed transitions file(s); $N_{HRstates}$: number of states with uncertainties $\leqslant 0.01$ cm^{-1}; $N_{HRlines}$: number of lines in the ExoMolHR data set with $R > 100{,}000$; $Size_{HR}$: file size of the uncompressed ExoMolHR data set; ExoMol line list: data source reference.

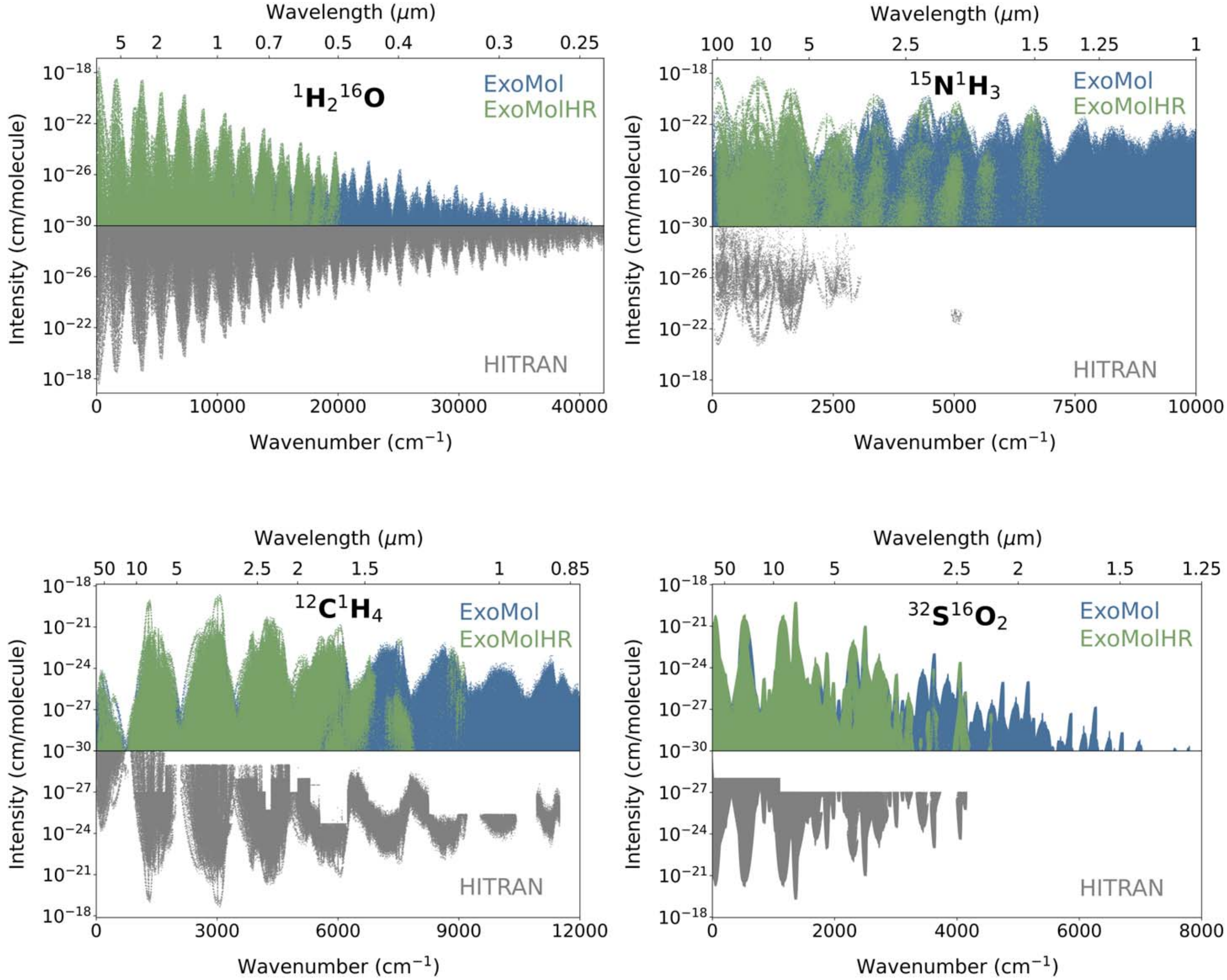

Figure 3. Comparison of the line intensities (cm molecule^{-1}) from ExoMol, ExoMolHR (top), and HITRAN (bottom) databases at $T = 296$ K of $^1H_2^{16}O$, $^{15}N^1H_3$, $^{12}C^1H_4$, and $^{32}S^{16}O_2$. The highlighted points in the upper panels show intensities provided by ExoMolHR, while the darker background shows the full coverage given by the POKAZATEL, CoYuTe-15, MM, and ExoAmes line lists of $^1H_2^{16}O$, $^{15}N^1H_3$, $^{12}C^1H_4$, and $^{32}S^{16}O_2$, respectively.

doing so, which helps reduce the likelihood of erroneous downloads.

4.4. Database Summary and Sources

Table 8 displays a list of molecules, isotopologues, data sets, and their corresponding versions (update date) and data sources. The number of initial states in the ExoMol database `.states` file as a data source and the number of the states with lower uncertainty ($\leqslant 0.01$ cm^{-1}) used in the ExoMolHR database are compared in this table. Similarly, Table 8 lists the number of transitions contained the `.trans` file in the ExoMol database and the total number of transitions and file size for each data set compared to the final line list number and file size in the ExoMolHR database.

5. Comparisons and Discussion

Fifteen of the 33 species currently considered by ExoMolHR are also present in the HITRAN database (I. E. Gordon et al. 2022). To compare ExoMolHR results with its initial source database ExoMol and high-resolution database HITRAN, we present the following figures in this section calculated by a Python program PyExoCross (J. Zhang et al. 2024). To mimic HITRAN, we only consider those lines whose intensities are larger than 10^{-30} cm molecule^{-1} at $T = 296$ K. As can be seen, the coverage provided by ExoMolHR is generally more complete than that provided by HITRAN.

Figure 3 compares the intensities of H_2O, NH_3, CH_4, and SO_2 obtained from the 2024 release of ExoMol (J. Tennyson et al. 2024b), ExoMolHR, and the 2020 release of HITRAN (I. E. Gordon et al. 2022) databases. These intensities (cm molecule^{-1}) are calculated at a temperature of 296 K, covering the entire wavenumber range in cm^{-1}. The line lists from the ExoMolHR and ExoMol databases are POKAZATEL of $^1H_2^{16}O$ (O. L. Polyansky et al. 2018), CoYuTe-15 of $^{15}N^1H_3$ (S. N. Yurchenko et al. 2024a), MM of $^{12}C^1H_4$ (S. N. Yurchenko et al. 2024d), and ExoAmes of $^{32}S^{16}O_2$ (D. S. Underwood et al. 2016). By comparison of the distribution of the ExoMolHR and HITRAN points with the ExoMol points in this figure, it is evident that high-resolution spectra are

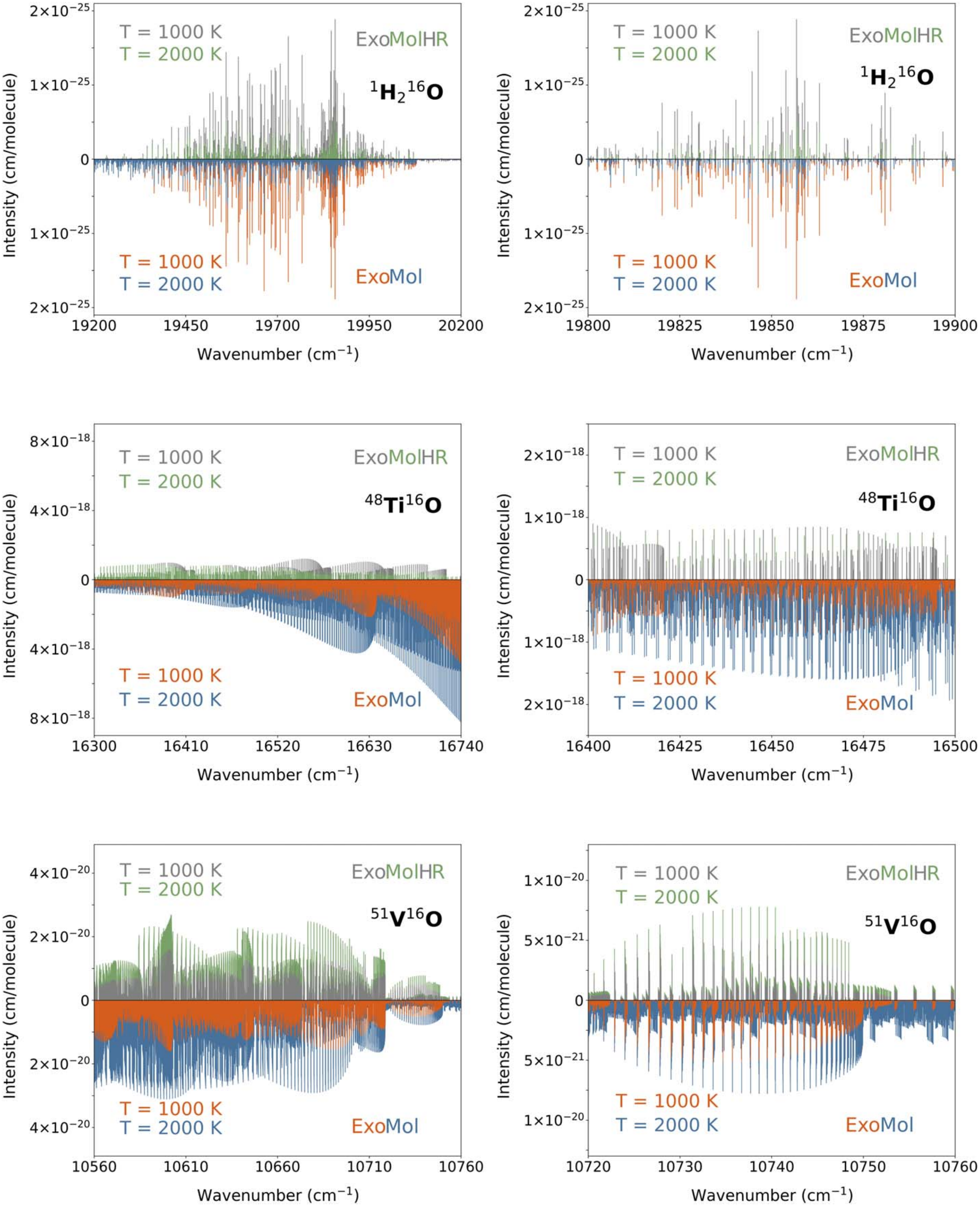

Figure 4. Comparison of the line intensities (cm molecule^{-1}) from ExoMolHR (top) and ExoMol (bottom) databases at temperatures $T = 1000$ and 2000 K of $^{1}H_2^{16}O$, $^{48}Ti^{16}O$, and $^{51}V^{16}O$.

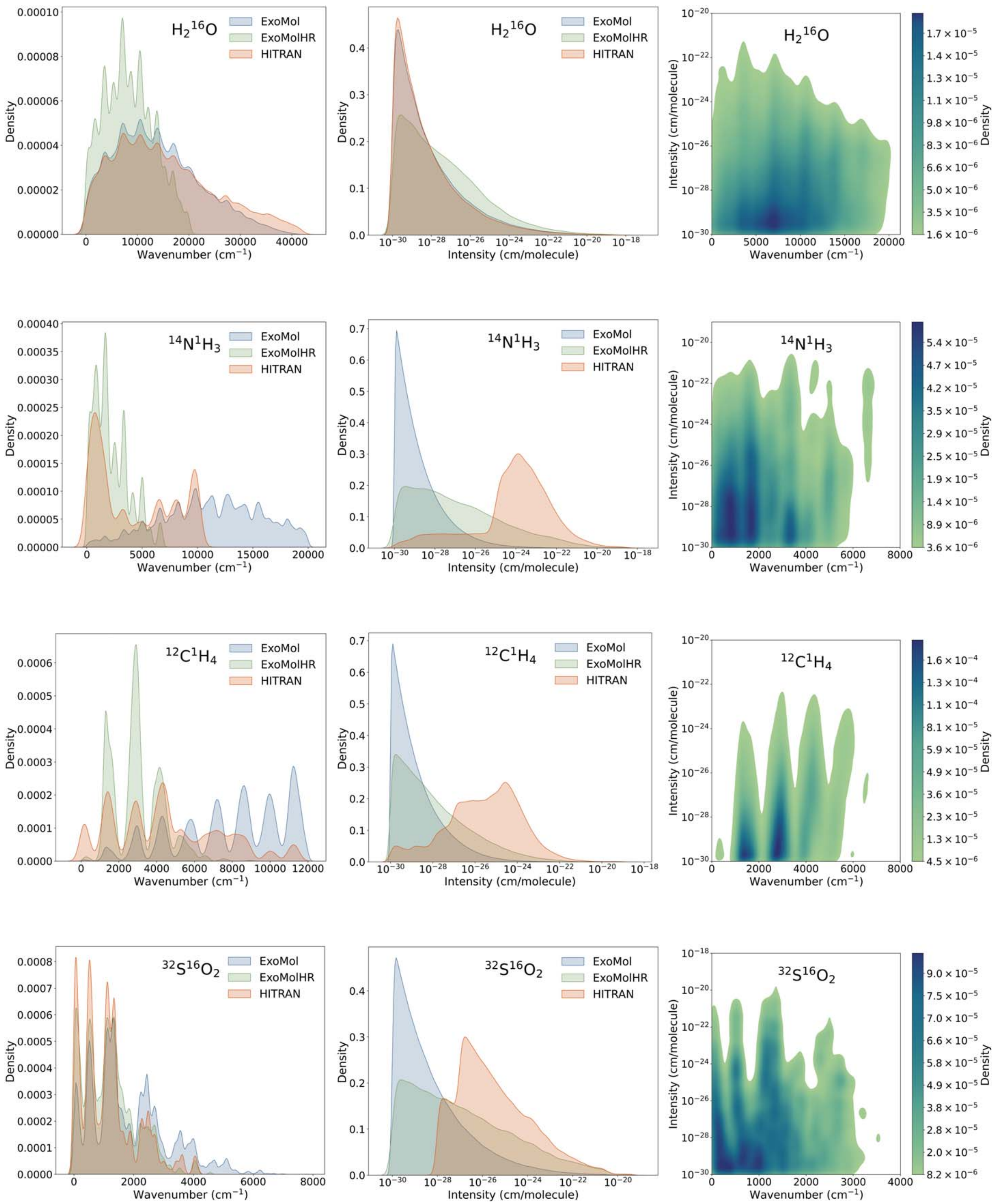

Figure 5. Compare the densities of wavenumbers (left) and line intensities (middle) of the ExoMol, ExoMolHR, and HITRAN databases at $T = 296$ K for $^{1}H_2^{16}O$, $^{14}N^{1}H_3$, $^{12}C^{1}H_4$, and $^{32}S^{16}O_2$. The ExoMol line lists provide full coverage using the POKAZATEL, CoYuTe, MM, and ExoAmes line lists of $^{1}H_2^{16}O$, $^{14}N^{1}H_3$, $^{12}C^{1}H_4$, and $^{32}S^{16}O_2$, respectively. The 2D plots of the densities between wavenumbers and line intensities (cm molecule^{-1}) for ExoMolHR databases at $T = 296$ K are displayed on the right panels.

generally distributed in the low-wavenumber range at room temperature. When comparing the distribution of the ExoMolHR and HITRAN points, we observe that high-resolution spectra with low uncertainty are primarily concentrated in the low-wavenumber region.

Figure 4 presents a comparative analysis of the intensities (cm molecule^{-1}) for H_2O (O. L. Polyansky et al. 2018) derived from the ExoMol and ExoMolHR databases at two distinct temperatures, $T = 1000$ and 2000 K, focused on the wavenumber range of [19,200, 20,200] cm^{-1}. It also provides a detailed examination within the narrower interval of [19,800, 19,900] cm^{-1}. Similar comparisons are given for $^{48}Ti^{16}O$ (L. K. McKemmish et al. 2019, 2024) and $^{51}V^{16}O$ (C. A. Bowesman et al. 2024; L. K. McKemmish et al. 2024); these species are not considered in the HITRAN database. It can be seen that for TiO and VO, the ExoMolHR coverage is patchier than for the better-studied HITRAN molecules. Better coverage of the high-resolution lines for these species will require new high-resolution spectroscopic measurements.

To analyze the distribution of the high-resolution line list among the range of the wavenumbers and intensities, we use $^{1}H_2^{16}O$, $^{14}N^{1}H_3$, $^{12}C^{1}H_4$, and $^{32}S^{16}O_2$ as samples in Figure 5. The left panel shows the densities for points in Figure 3 among the wavenumber ranges for the ExoMol, ExoMolHR, and HITRAN databases. The left panel illustrates the relationship between the distribution density of spectral-line points and the wavenumbers at room temperature. It is observed that compared to the comprehensive data set provided by the ExoMol database, the spectra from the high-resolution databases ExoMolHR and HITRAN are predominantly concentrated in the lower-wavenumber region. The middle panel reveals that, after filtering out low-resolution and high-uncertainty line lists from the ExoMol database, there is a significant reduction in the density of low-intensity spectral lines for the ExoMolHR database; we note that omitting such transitions can have a profound effect on the opacity (S. N. Yurchenko et al. 2014). The right panel provides a more intuitive representation of the density distribution of high-resolution spectra by depicting the relationship between wavenumber and intensity in the two-dimensional plots. These plots show that a higher concentration of points is present in the lower-wavenumber range and lower-intensity region. However, few high-resolution and higher-intensity spectra are distributed in the high-wavenumber region.

6. Conclusions

ExoMolHR is a new high-resolution molecular spectroscopic database, developed from the ExoMol database, which is designed for high-temperature molecular line lists for modeling exoplanet atmospheres. The ExoMolHR database is based on resolving power calculated by filtering out states whose energies are only known with high uncertainty; transition wavenumber/wavelengths known to better than 1 part in 100,000 are subsequently extracted to give high-resolution line lists. The ExoMolHR database contains 24,307,135 transitions associated with 238,263 states that have been determined with low uncertainties ($\Delta E \leqslant 0.01$ cm^{-1}) from 727,841,563,143 transitions and 129,237,384 states for the same data sets as in the ExoMol database. We note that our procedure will inevitably lead to missing lines in the ExoMolHR compilation. Users who wish to check for missing lines or to looking for completeness should use the original ExoMol line lists with one of the spectral generator programs ExoCross (S. N. Yurchenko et al. 2018) or PyExoCross (J. Zhang et al. 2024).

The ExoMolHR website allows users to select molecules and isotopologues, calculate intensities based on user-specified temperatures, and apply filters with the desired wavenumber range and intensity threshold. The website provides a download link for a compressed folder containing the high-resolution line lists in .csv format for each isotopologue, along with the total folder size and the number of whole line lists. Additionally, the site provides a spectral viewer which generates stick spectra for all selected isotopologues within the specified temperature, wavenumber range, and intensity threshold. The web page also offers interactive zooming and panning functionality for the spectral plot. The ExoMolHR database is freely accessible through an interactive web interface at https://www.exomol.com/exomolhr/. An API has been designed to facilitate user data requests, with the option to dynamically access and view data directly on the website.

The molecular data in the ExoMolHR database are derived from the ExoMol database, with the low-uncertainty line lists computed using data from the MARVEL database. At the time of writing, the ExoMolHR database supports 58 isotopologues from 33 molecules and this number is increasing as additional MARVEL studies are completed.

Acknowledgments

This work was supported by the European Research Council (ERC) under Advanced Investigator Project 883830 and by UK STFC under grant ST/Y001508/1.

Data Availability

The data that support the findings of this study are openly available at https://www.exomol.com/exomolhr/. The molecular line lists sources discussed in this paper are available from the ExoMol website https://www.exomol.com/. The PyExoCross program used for calculating in this study is publicly accessible on GitHub at https://github.com/ExoMol/PyExoCross.git and its program manual web page is https://pyexocross.readthedocs.io/.

Software: PyExoCross (J. Zhang et al. 2024).

ORCID iDs

Jingxin Zhang https://orcid.org/0000-0002-6374-6251
Christian Hill https://orcid.org/0000-0001-6604-0126
Jonathan Tennyson https://orcid.org/0000-0002-4994-5238
Sergei N. Yurchenko https://orcid.org/0000-0001-9286-9501

References

Al-Derzi, A. R., Yurchenko, S. N., Tennyson, J., et al. 2021, JQSRT, 266, 107563
Al-Refaie, A. F., Yurchenko, S. N., Yachmenev, A., & Tennyson, J. 2015, MNRAS, 448, 1704
Azzam, A. A. A., Yurchenko, S. N., Tennyson, J., & Naumenko, O. V. 2016, MNRAS, 460, 4063
Barton, E. J., Hill, C., Czurylo, M., et al. 2017, JQSRT, 203, 490
Bernath, P. F. 2020, JQSRT, 240, 106687
Bowesman, C. A., Akbari, H., Hopkins, S., Yurchenko, S. N., & Tennyson, J. 2022, JQSRT, 289, 108295
Bowesman, C. A., Qu, Q., McKemmish, L. K., Yurchenko, S. N., & Tennyson, J. 2024, MNRAS, 529, 1321
Bowesman, C. A., Mizus, I. I., Zobov, N. F., et al. 2023, MNRAS, 519, 6333

Bowesman, C. A., Shuai, M., Yurchenko, S. N., & Tennyson, J. 2021, MNRAS, 508, 3181
Brady, R. P., Yurchenko, S. N., Tennyson, J., & Kim, G.-S. 2024, MNRAS, 527, 6675
Buldyreva, J., Stehlin, K., Yurchenko, S. N., Guest, E. R., & Tennyson, J. 2025, ApJS, 276, 23
Chubb, K. L., Tennyson, J., & Yurchenko, S. N. 2020, MNRAS, 493, 1531
Coles, P. A., Yurchenko, S. N., & Tennyson, J. 2019, MNRAS, 490, 4638
Darby-Lewis, D., Tennyson, J., Yurchenko, S. N., & Lawson, K. D. 2020, JPhB, 53, 135202
Endres, C. P., Schlemmer, S., Schilke, P., Stutzki, J., & Müller, H. S. P. 2016, JMoSp, 327, 95
Furtenbacher, T., Császár, A. G., & Tennyson, J. 2007, JMoSp, 245, 115
Germann, M., Hjalten, A., Tennyson, J., et al. 2024, JQSRT, 312, 108782
Gordon, I. E., Rothman, L. S., Hargreaves, R. J., et al. 2022, JQSRT, 277, 107949
Guest, E. R., Tennyson, J., & Yurchenko, S. N. 2024, JMoSp, 401, 111901
Hargreaves, R. J., Gordon, I. E., Rothman, L. S., et al. 2019, JQSRT, 232, 35
Hill, C., & Hanicinec, M., 2022 A Python Package for Managing Simple Chemical Species and States, v2.8.0, GitHub, https://github.com/xnx/pyvalem
Jørgensen, U. G., Larsson, M., Iwamae, A., & Yu, B. 1996, A&A, 315, 204
Kefala, K., Boudon, V., Yurchenko, S. N., & Tennyson, J. 2024, JQSRT, 316, 108897
Kramida, A., Ralchenko, Y., Reader, J. & NIST ASD Team 2020, Atoms, 8, 56
Kramida, A., Ralchenko, Y., Reader, J. & NIST ASD Team 2015, NIST Atomic Spectra Database, v5.3, (Gaithersburg, MD: National Institute of Standards and Technology), http://physics.nist.gov/asd
Kurucz, R. L. 2011, CaJPh, 89, 417
McKemmish, L. K., Bowesman, C. A., Kefala, K., et al. 2024, RASTI, 3, 565
McKemmish, L. K., Masseron, T., Hoeijmakers, J., et al. 2019, MNRAS, 488, 2836
McKemmish, L. K., Syme, A. M., Borsovszky, J., et al. 2020, MNRAS, 497, 1081
Mellor, T., Owens, A., Yurchenko, S. N., & Tennyson, J. 2022, MNRAS, 520, 1997
Owens, A., Dooley, S., McLaughlin, L., et al. 2022a, MNRAS, 511, 5448
Owens, A., Mitrushchenkov, A., Yurchenko, S. N., & Tennyson, J. 2022b, MNRAS, 516, 3995
Owens, A., Wright, S. O. M., Pavlenko, Y., et al. 2024a, MNRAS, 527, 731
Owens, A., Yurchenko, S. N., & Tennyson, J. 2024b, MNRAS, 530, 4004
Perri, A. N., & McKemmish, L. K. 2024, MNRAS, 531, 3023
Perri, A. N., Taher, F., & McKemmish, L. K. 2023, MNRAS, 524, 4631
Pezoa, F., Reutter, J. L., Suarez, F., Ugarte, M., & Vrgoč, D. 2016, in Proc. of the 25th Int. Conf. on World Wide Web (Geneva: International World Wide Web Conferences Steering Committee), 263
Pickett, H. M., Poynter, R. L., Cohen, E. A., et al. 1998, JQSRT, 60, 883
Polyansky, O. L., Kyuberis, A. A., Zobov, N. F., et al. 2018, MNRAS, 480, 2597
Qu, Q., Yurchenko, S. N., & Tennyson, J. 2021, MNRAS, 504, 5768
Rothman, L. S., Gordon, I. E., Barber, R. J., et al. 2010, JQSRT, 111, 2139
Ryabchikova, T., Piskunov, N., Kurucz, R. L., et al. 2015, PhyS, 90, 054005
Semenov, M., Clark, N., & Yurchenko, S. N. 2022, MNRAS, 516, 1158
Semenov, M., El-Kork, N., Yurchenko, S. N., & Tennyson, J. 2025, MNRAS, 536, 714
Syme, A.-M., & McKemmish, L. K. 2021, MNRAS, 505, 4383
Tennyson, J., Furtenbacher, T., Yurchenko, S. N., & Császár, A. G. 2024a, JQSRT, 316, 108902
Tennyson, J., Hill, C., & Yurchenko, S. N. 2013, in AIP Conf. Proc. 1545, 6th Int. Conf. Atomic and Molecular Data and their Applications ICAMDATA-2012, ed. J. D. Gillaspy, W. L. Wiese, & Y. A. Podpaly (Melville, NY: AIP), 186
Tennyson, J., & Yurchenko, S. N. 2012, MNRAS, 425, 21
Tennyson, J., Yurchenko, S. N., Al-Refaie, A. F., et al. 2016, JMoSp, 327, 73
Tennyson, J., Yurchenko, S. N., Al-Refaie, A. F., et al. 2020, JQSRT, 255, 107228
Tennyson, J., Yurchenko, S. N., Zhang, J., et al. 2024b, JQSRT, 326, 109083
Underwood, D. S., Tennyson, J., Yurchenko, S. N., et al. 2016, MNRAS, 459, 3890
Watson, J. K. G. 1984, JMoSp, 103, 350
Yurchenko, S. N., Al-Refaie, A. F., & Tennyson, J. 2018, A&A, 614, A131
Yurchenko, S. N., Bowesman, C. A., Brady, R. P., et al. 2024a, MNRAS, 533, 3442
Yurchenko, S. N., Brady, R. P., Tennyson, J., et al. 2024b, MNRAS, 527, 4899
Yurchenko, S. N., Mellor, T., & Tennyson, J. 2024c, MNRAS, 534, 1364
Yurchenko, S. N., Mellor, T. M., Freedman, R. S., & Tennyson, J. 2020a, MNRAS, 496, 5282
Yurchenko, S. N., Nogué, E., Azzam, A. A. A., & Tennyson, J. 2023, MNRAS, 520, 5183
Yurchenko, S. N., Owens, A., Kefala, K., & Tennyson, J. 2024d, MNRAS, 528, 3719
Yurchenko, S. N., Szajna, W., Hakalla, R., et al. 2024e, MNRAS, 527, 9736
Yurchenko, S. N., Tennyson, J., Bailey, J., Hollis, M. D. J., & Tinetti, G. 2014, PNAS, 111, 9379
Yurchenko, S. N., Tennyson, J., Miller, S., et al. 2020b, MNRAS, 497, 2340
Yurchenko, S. N., Tennyson, J., Syme, A.-M., et al. 2022, MNRAS, 510, 903
Zhang, J., Tennyson, J., & Yurchenko, S. N. 2024, RASTI, 3, 257